

**Michael C. Breadmore**

Australian Centre  
for Research on  
Separation Science,  
School of Chemistry,  
University of Tasmania,  
Hobart, Tasmania, Australia

Received October 1, 2007  
Revised December 6, 2007  
Accepted December 6, 2007

## Research Article

# Unlimited-volume stacking of ions in capillary electrophoresis. Part 1: Stationary isotachophoretic stacking of anions

An online technique for stacking based on the generation of a stationary isotachophoretic (sITP) boundary is presented. By balancing the anodic migration of an ITP boundary with a cathodic EOF, a stationary boundary is formed that can be used to indefinitely concentrate analytes according to ITP principles during electrokinetic injection. The ITP boundary is created by using an electrolyte containing a leading ion (chloride) and a suitable terminating ion added to the sample (2-morpholinoethanesulphonic acid, MES). Destacking and separation are achieved simply by replacement of the sample vial with electrolyte. The formation and stabilisation of the sITP boundary were evaluated through computer simulation which revealed that the pH had little impact upon the formation of the sITP boundary, but did govern the position at which it becomes stationary. Simulations also demonstrated that similar results were obtained when the capillary was initially filled with sample/terminator or leader/electrolyte, which was also supported by experimental results. Using 100 mM  $\text{Cl}^-$ , 200 mM Tris, pH 8.05 as the leader/electrolyte and adding 100 mM MES, 200 mM Tris, pH 8.05 to the sample, the sITP boundary was established after 5 min at  $-20$  kV and was stable for at least 60 min. This provided detection limits for  $\text{NO}_2^-$ ,  $\text{NO}_3^-$  and  $\text{SCN}^-$  of 0.05–0.66 ppb, which are 10 000 times lower than hydrodynamic injection and 10–50 times lower than other stacking approaches used for these inorganic ions.

**Keywords:**

Inorganic anions / Isotachopheresis / Preconcentration / Unlimited stacking

DOI 10.1002/elps.200700728

## 1 Introduction

One of the most cited limitations of CE is the higher concentration LOD when it is compared to more conventional HPLC. This has led to a number of strategies for online concentration over the last 20 years (see recent reviews for a full overview [1–5]), and includes various stacking approaches such as field-amplified sample stacking (FASS) [6, 7], ITP [8, 9], dynamic pH junction [10, 11] and pH-mediated sample stacking [12, 13]. While these allow the injection of large volumes of sample and offer a significant improvement in sensitivity over a normal injection, they are restricted because the sample volume is physically limited by the volume of the capillary. This can be partially overcome by the use of

electrokinetic injection (to give field-amplified sample injection, FASI also called field-enhanced sample injection, FESI [14, 15], or electrokinetic supercharging [16]) which can generally increase the sensitivity by up to 1000. Quirino and Terabe [17] combined electrokinetic injection with sweeping to improve the sensitivity by almost 1 000 000 in an approach they called anion-exhaustive selective injection – sweeping (AESI-sweep). The sweeping step was employed to restack analytes that had broadened during electrokinetic injection. While this is impressive, it relies on the use of two stacking mechanisms to achieve this improvement and some analytes are difficult to concentrate by one, let alone two different methods.

More recently, Jung *et al.* [18, 19] have demonstrated improvements in sensitivity over 500 000 using electrokinetic injections under field-amplified ITP conditions on a microchip. This work is similar to that originally published by Jandik and Jones [20] in the early 1990's in which a low concentration of terminating ion was added to the sample to facilitate ITP stacking during electrokinetic injection. While the results obtained by Jung *et al.* are more impressive than Jandik and Jones, this approach is limited in that the stacking boundary continues to move towards the detector during

---

**Correspondence:** Dr. Michael C. Breadmore, Australian Centre for Research on Separation Science, School of Chemistry, University of Tasmania, GPO Box 252-75, Hobart, Tasmania 7001, Australia  
**E-mail:** mcb@utas.edu.au  
**Fax:** +61-3-6226-2858

**Abbreviations:** FESI, field-enhanced sample injection; sITP, stationary isotachophoretic

continued injection, thus limiting both the subsequent separation and also the potential sensitivity enhancement that can be gained.

One way that these limitations can be overcome is to apply an opposing force to capture and hold analytes during long injections potentially allowing an infinite amount of sample to be injected. The simplest and most obvious approach is to apply a hydrodynamic counterflow, an approach first reported by Preetz in the 1960's [21, 22] and built upon by Everaerts *et al.* in 1976 [23]. A very recent publication by Shackman and Ross [24] demonstrated an improvement in sensitivity of 100 000 with an 8 min injection using short capillary counter-pressure ITP. With regard to ITP stacking as a precursor to a subsequent CE separation (termed single capillary ITP-CE), there have been only a few reports of the application of a hydrodynamic counter pressure during the ITP stage [25–30]; In these instances, the sample was injected by hydrodynamic pressure and the counter pressure applied during the ITP focusing stage to remove the terminator from the capillary and position the stacked zones at the capillary inlet. Urbánek *et al.* [31] applied a counter pressure with continuous electrokinetic injection in an effort to enhance sensitivity, however they found that the application of high counter pressures resulted in a loss of efficiency due to the parabolic profile of the hydrodynamic flow.

Recently, Gong *et al.* [32] published a novel and innovative approach for the concentration of charged and neutral components based on sweeping. In their approach, the sweeping front was held stationary by balancing the electrophoretic velocity of the micelles with the EOF. This was achieved by using the cationic surfactant dodecyltrimethylammonium bromide, which partially coated the capillary to regulate the EOF and hence cause the sweeping boundary to become stationary while maintaining the majority of the capillary length for subsequent separation. This allowed target analytes to be injected from the sample and accumulate at the stationary sweeping front from multiple column volumes of sample, potentially allowing unlimited stacking. Using this approach, the authors were able to demonstrate sensitivity enhancements of 4000–5000 with 60 min, –20 kV injections. Following this work, Horakova *et al.* [33] presented a similar concept which they described as 'electrokinetic accumulation'. This system involved the continuous electrokinetic injection of benzoic and sorbic acids which were accumulated on a pH boundary created between the high pH sample and low pH electrolyte. Accumulated analytes (which were neutral) were mobilised and separated by sweeping of the stacked zones with micelles. An improvement in sensitivity of 4600 was achieved with a 120 min injection.

In this work, a stationary isotachophoretic (sITP) boundary is created by balancing the electrophoretic migration of the ITP boundary with that of the EOF to allow the continuous stacking of ions during electrokinetic injection. The evolution and stabilisation of the boundary are exam-

ined in detail through computer simulation, and experimentally verified by CE using a mixture of simple inorganic anions. This is the first demonstration of the use of the EOF to counter movement of an ITP boundary during continuous electrokinetic injection in CE.

## 2 Materials and methods

### 2.1 Computer simulations

The computer program used for simulating stacking conditions has been presented previously in various configurations and is based upon the model of Bier *et al.* [34] with the mathematical model and the construction of the numerical simulation scheme presented in Saville and Palusinski [35] and Palusinski *et al.* [36], respectively. The simulator for high-resolution simulations [37–40] was employed together with a newly developed modification which accounts for changing boundary conditions at the column ends which has been described previously [41]. This simulator includes *in situ* calculation of the EOF using wall titration data as an input. The program was implemented on Itanium2 1.6 GHz processors housed in the Tasmanian Partnership for Advanced Computing (TPAC) and Australian Partnership for Advanced Computing (APAC) facilities.

The total capillary length was 50 mm (5 cm) and was divided into 20 000 equal segments. Simulations were performed at a constant voltage of 2000 V (400 V/cm), approximating the application of 10 kV over a 25 cm capillary. Current densities were in the order of 17 000–23 000 A/m<sup>2</sup> which are representative of practical current densities. Sample-electrolyte boundaries were defined at positions 5 mm from the inlet or outlet end of the capillary with an initial width set at 0.1% of the capillary length, or 0.05 mm (50 μm). All simulations were for a time of 10 min with data collection of 101 data points, or every 0.1 min except for construction of the detection trace for destacking/separation. Simulations of the destacking/separation phase were performed by manually editing the input file to be consistent with changing the inlet vial from sample to electrolyte at a position of 5 mm from the end of the capillary. Continuation runs were conducted at constant voltage (2000 V, 400 V/cm) and data was saved every 0.01 min to allow construction of the detection trace. The detection trace was generated at 47.5 mm from the inlet (segment number 19 000) with the detector response for all analytes set to 1.

Mobility data for the ions was obtained from previously published results [42].

### 2.2 Apparatus

All experiments were performed with an Agilent HP<sup>3D</sup>CE (Agilent Technologies, Waldbronn, Germany) and polyimide-coated fused-silica capillary (Phoenix, AZ, USA) of 25 μm id with a length of 34.5, 26.0 cm to the detector unless

otherwise stated. Detection was performed using the inbuilt DAD at 214 nm unless otherwise stated. All separations were performed with the capillary thermostated at 25°C.

### 2.3 Chemicals

Analytical-grade Tris and 2-morpholinoethanesulphonic acid (MES) were from Sigma–Aldrich (Milwaukee, USA). HCl was from BDH (Kilsyth, Vic, Australia).

Leading electrolytes were prepared by dilution of HCl to 100 mM and the pH adjusted to pH 8.05 with Tris. Terminating electrolytes were prepared from MES also at a concentration of 100 mM, and the pH adjusted to pH 8.05 with Tris.

All analytes were obtained as analytical grade sodium or potassium salts from Sigma–Aldrich. Stock solutions were prepared at a concentration of 1000 ppm and diluted in terminating electrolyte as required.

### 2.4 Electrophoresis

New capillaries were conditioned with 1 M NaOH for 60 min prior to use and daily with 0.1 M NaOH for 10 min, H<sub>2</sub>O for 10 min and leading electrolyte for 10 min. Between separations the capillary was conditioned with leading electrolyte for 2 min.

Injection using a sITP boundary was performed by placing the sample in the inlet vial and applying voltage for a designated time. After injection the inlet vial was changed to the leading electrolyte/terminator and the voltage applied for

separation. Prior to application of the sITP injection voltage, the capillary was either filled with sample (in the terminating electrolyte) or with leading electrolyte. During separations, injection and changing vials was performed using the time-table function in the chemstation software to allow the absorbance data to be saved during injection.

## 3 Results and discussion

The underlying premise of sITP stacking is the generation of an ITP boundary that it is *stationary* and will stack analytes during long electrokinetic injections of sample. While the ITP boundary can be held stationary by application of a counter-pressure, this cannot necessarily be achieved with commercial instrumentation, requires very accurate control of the pressure and suffers from decreased efficiency due to the nature of hydrodynamic flow. The use of EOF can avoid these limitations, and this has been successfully employed by Gong *et al.* [32] who balanced electrophoretic migration of a sweeping front with the EOF. In this work a sITP boundary has been created using a similar approach to that described by Thormann *et al.* [43] during the investigation of ITP processes in unmodified fused-silica capillaries.

Figure 1 shows a schematic representation of the steps involved in the sITP stacking system developed in this work. The capillary is initially filled with leader/electrolyte while the sample contains the terminator ion (Fig. 1a). Application of a negative voltage (Fig. 1b) causes the EOF to be generated towards the inlet vial (cathode), while the ITP boundary

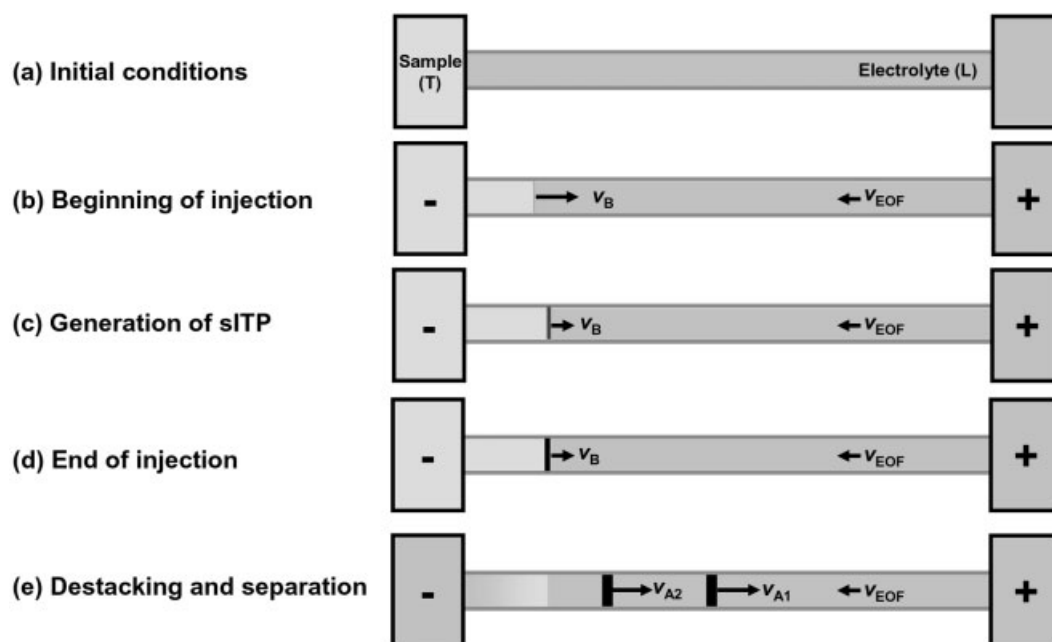


**Figure 1.** Schematic representation of continuous injection and stacking using a sITP boundary. L is the leading ion, T is the terminating ion,  $v_B$  is the velocity of the boundary,  $v_{EOF}$  is the velocity of the EOF,  $v_{A1}$  and  $v_{A2}$  are the velocities of analytes A1 and A2.

moves towards the outlet vial (anode). As more of the capillary becomes filled with sample/terminator, the velocity of the boundary,  $v_B$  gradually decreases, while the magnitude of the EOF,  $v_{EOF}$  increases until the two velocities are exactly equal in magnitude, but of opposite direction (Fig. 1c) thus creating a sITP boundary. At this stage it is possible to continuously inject analyte from the sample into the sITP zone which will continue to stack according to ITP principles (Fig. 1d). At the end of sample injection, the sITP boundary must be destroyed to allow the analytes to separate, which can be achieved by changing the sample inlet vial to the electrolyte/leader. The sITP boundary destabilises due to migration of the leader through ITP zones and the stacked analytes can be separated according to conventional CZE (Fig. 1e).

A more detailed understanding of the mechanism through which a sITP boundary is generated can be gained from Fig. 2. This figure shows the distribution of leader and terminator ions along the capillary every 0.5 min from 0 to 2.5 min using conditions similar to that demonstrated by Thormann *et al.* [43] in their report on ITP in unmodified fused-silica capillaries. It can be seen that a sharp steady-state ITP boundary is created between the leader and terminating ions after 0.5 min, with the concentration of terminating ion being lower than that of the leader due to the Kohlrausch regulating function. This steady-state ITP boundary migrates towards the cathode until it becomes sta-

tionary when the velocity of the boundary is balanced by the velocity of the EOF. It is very important to note that this boundary only becomes stationary due to a concurrent change in the EOF brought about by movement of the boundary through the capillary. This can also be seen from Fig. 2 which shows the localised EOF along the capillary with a sharp discontinuity either side of the steady-state ITP boundary, with a higher EOF observed in the terminating electrolyte and a lower EOF in the leading electrolyte. As the boundary moves through the capillary and it becomes filled with more terminating electrolyte, the total EOF through the capillary increases which decreases the cathodic movement of the ITP boundary. In this way as the ITP boundary slowly migrates through the capillary the EOF gradually increases until it perfectly balances the ITP boundary velocity thus creating a sITP boundary.

### 3.1 Conditions to generate a sITP boundary

As mentioned above, once the ITP boundary has been generated the boundary velocity must be perfectly balanced by the EOF to create a sITP boundary. In the work of Thormann *et al.* [43], anionic ITP boundaries between chloride and salicylate were observed to become stationary at a position of 40–90% of the capillary length at a pH of 5–6. Given that this was undertaken at pH 5–6, a stronger EOF would be anticipated at higher pH which should cause the sITP boundary to

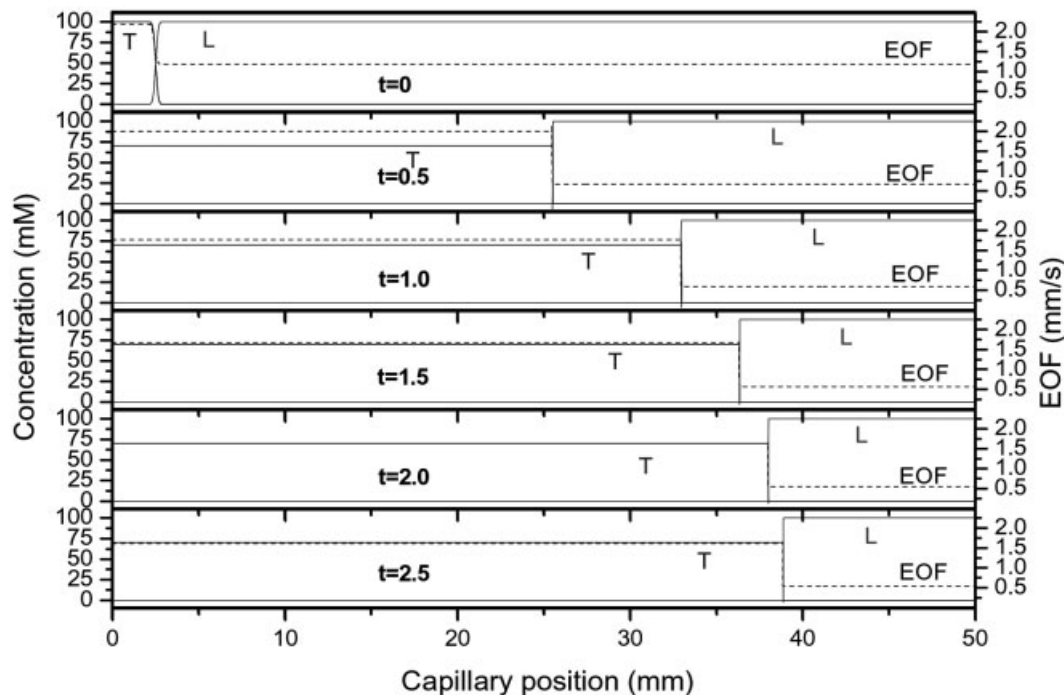


**Figure 2.** Computer simulations showing the leader (L), terminator (T) and EOF profiles along the capillary every 0.5 min during the generation of a sITP boundary. Computer simulations were performed at 400 V/cm with 100 mM  $\text{Cl}^-$  ( $\mu_{ep} = -80 \times 10^{-9} \text{ m}^2/\text{V}\cdot\text{s}$ ) as the leading electrolyte and terminator and 100 mM  $\text{C}_8\text{SO}_3^-$  ( $\mu_{ep} = -28 \times 10^{-9} \text{ m}^2/\text{V}\cdot\text{s}$ ) as the terminating electrolyte both buffered with a weak base ( $\mu_{ep} = 28 \times 10^{-9} \text{ m}^2/\text{V}\cdot\text{s}$ ,  $pK_a$  4–8). All other conditions are described in Section 2.

become stationary closer to the inlet of the capillary, although too strong an EOF would cause the boundary to be removed from the capillary. To examine the effect of EOF on the position of the sITP boundary, computer simulations were performed to monitor the evolution of the sITP boundary throughout sample injection using a number of simple inorganic anions. These ions were selected due their good UV detector response and the fact that they have a high electrophoretic mobility and should therefore migrate faster than the EOF during the subsequent CZE separation. Figure 3 shows the results of these simulations by monitoring the position of  $\text{SCN}^-$  ( $\mu_{\text{ep}} = -63 \times 10^{-9} \text{ m}^2/\text{V}\cdot\text{s}$ ) during the stacking process using 100 mM  $\text{Cl}^-$  as the leading electrolyte ( $\mu_{\text{ep}} = -76 \times 10^{-9} \text{ m}^2/\text{V}\cdot\text{s}$ ) and 100 mM  $\text{C}_8\text{SO}_3^-$  as the terminating electrolyte ( $\mu_{\text{ep}} = -28 \times 10^{-9} \text{ m}^2/\text{V}\cdot\text{s}$ ), selected due to its previous use in ITP preconcentration by Jandik and Jones [20]. At each pH condition, the electrolyte was buffered by using a theoretical base that had a  $\text{pK}_a$  value of 4–8 and a concentration of 200 mM. At the beginning of these simulations (time 0 in each panel),  $\text{SCN}^-$  is positioned in the inlet vial and also in the capillary to the left of the 5 mm position. Upon application of the voltage, a steady-state ITP boundary is created between the leader and terminator ions, which allow analytes of intermediate mobility to be stacked accord-

ing to ITP principles as visualised by the sharp  $\text{SCN}^-$  peak in each of the panels. It can be seen that at a pH of 4 ( $\mu_{\text{EOF}} = 12.5 \times 10^{-9} \text{ m}^2/\text{V}\cdot\text{s}$ ), the ITP boundary moves through the entire capillary with the stacked  $\text{SCN}^-$  peak exiting the capillary after approximately 1 min. Under these conditions, the EOF is never sufficient to counter the movement of the ITP boundary. When the pH is increased to 5 ( $\mu_{\text{EOF}} = 31.0 \times 10^{-9} \text{ m}^2/\text{V}\cdot\text{s}$ ), a sITP boundary is created 40 mm along the capillary (80% of the capillary length) as evidenced by the  $\text{SCN}^-$  peak converging on a single position along the capillary. Increasing the pH further results in the  $\text{SCN}^-$  convergence point, and hence the sITP boundary, being closer towards the capillary inlet at a position of 16 mm (32% of the capillary length) when the pH is 7 ( $\mu_{\text{EOF}} = 50.9 \times 10^{-9} \text{ m}^2/\text{V}\cdot\text{s}$ ) and 8 ( $\mu_{\text{EOF}} = 52.5 \times 10^{-9} \text{ m}^2/\text{V}\cdot\text{s}$ ) as the EOF is larger at these pH values. Higher pH values were not examined as it is well known that the change in EOF above pH 8 is minimal and this would not have any significant influence on the position of the sITP boundary. These results suggest that careful control of the pH is not required to generate a sITP boundary, although it will govern the position at which the sITP boundary becomes stationary along the capillary and will therefore have an impact upon subsequent steps. It can also be concluded that a high pH

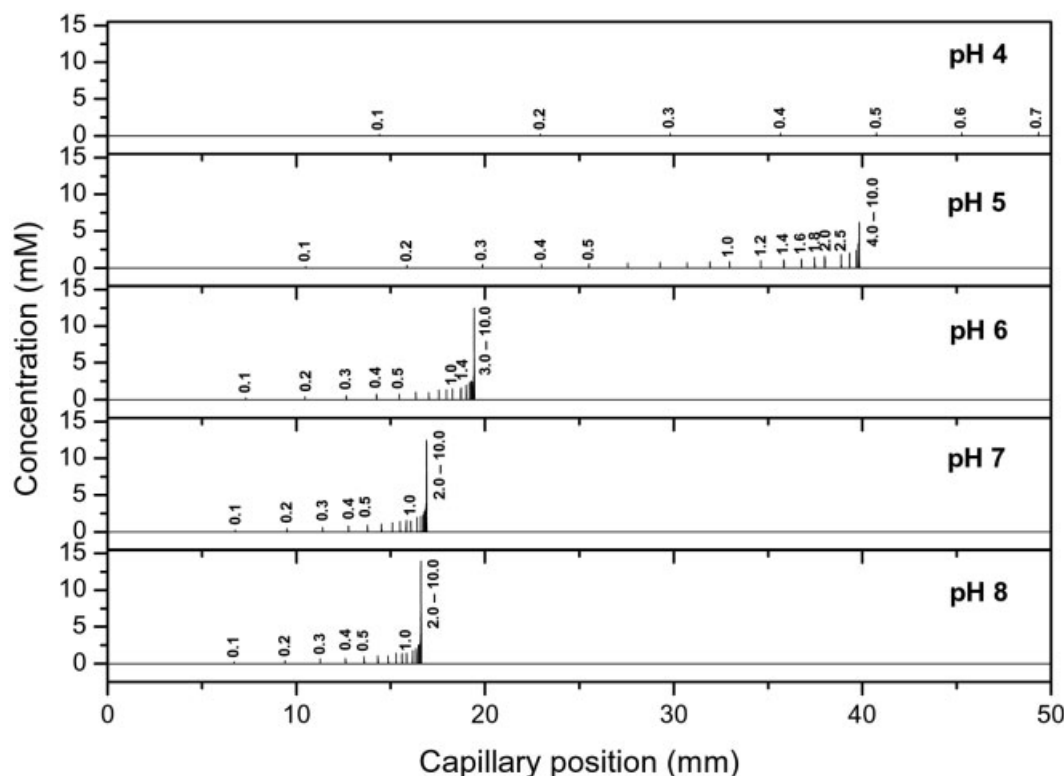


**Figure 3.** Computer simulation data showing the influence of pH (and hence EOF) on the generation and stabilization of the sITP boundary. Each panel shows the position of  $\text{SCN}^-$  every 0.1 min from 0 to 1 min, every 0.2 min from 1 to 2 min, every 0.5 min from 2 to 4 min and every 1.0 min from 4 to 10 min. Computer simulations were performed at 400 V/cm with 100 mM  $\text{Cl}^-$  ( $\mu_{\text{ep}} = -80 \times 10^{-9} \text{ m}^2/\text{V}\cdot\text{s}$ ) as the leading electrolyte and terminator and 100 mM  $\text{C}_8\text{SO}_3^-$  ( $\mu_{\text{ep}} = -28 \times 10^{-9} \text{ m}^2/\text{V}\cdot\text{s}$ ) as the terminating electrolyte both buffered with a weak base ( $\mu_{\text{ep}} = 28 \times 10^{-9} \text{ m}^2/\text{V}\cdot\text{s}$ ,  $\text{pK}_a$  4–8). All other conditions are described in Section 2.

(and hence high EOF) is beneficial as it maintains the sITP boundary closer to the capillary inlet thus leaving a greater amount of capillary length available for separation of the analytes once they are destacked. In all of the simulation results, except those conducted at pH 4, a sITP boundary was created, and the height of the peak increased considerably during continued injection, demonstrating the potential of sITP stacking for the concentration of anions.

The next stage in the use of a sITP boundary for continuous stacking is separation of the stacked zones after disruption of the ITP process. This is achieved by changing the inlet vial from sample/terminator to leader/electrolyte. The leading ion passes through the terminator zone and causes the steady-state ITP boundary to be disrupted and the stacked zones gradually destack and are separated according to their electrophoretic mobility. This is depicted in Fig. 4 which shows the profiles of the leader ( $\text{Cl}^-$ ) and terminator ( $\text{C}_8\text{SO}_3^-$ ) every 0.1 min after the inlet vial is changed from sample/terminator to leader/electrolyte. It can be seen that the steady-state ITP boundary is quickly dissipated by movement of the leading ion through the terminator zone. This results in the rapid destacking of the analytes from the ITP boundary, most easily seen from the inserts of each panel which show the  $\text{Cl}^-$  concentration in an expanded scale. As can be seen from these inserts, as the destacking proceeds, first one, then three peaks are separated from the ITP boundary. These destack in the order of  $\text{NO}_2^-$ ,  $\text{NO}_3^-$  and  $\text{SCN}^-$ , which is in order of decreasing electrophoretic mobility, *i.e.* the highest mobility ions are destacked first. Following destacking, these peaks are separated by conventional CZE and are easily separated from the terminating ion. It is important to note that these ions migrate to the detector against the EOF and therefore only ions that have an electrophoretic mobility sufficiently greater than the EOF can be detected. Examination of the simulation data also suggests that there is a slight change in the position of the ITP boundary along the column during destacking due to changes in electric field strength and the EOF, although this is not anticipated to have a significant influence on the resulting separation.

### 3.2 Experimental implementation of sITP stacking

To practically implement the sITP stacking system studied above a leading electrolyte of 100 mM  $\text{Cl}^-$  buffered at pH 8.05 with Tris was prepared, while a terminating electrolyte comprised 100 mM MES ( $\text{p}K_a$  6.05,  $\mu_{\text{ep}} = -28 \times 10^{-9} \text{ m}^2/\text{V}\cdot\text{s}$ ) buffered at pH 8.05 with Tris was also prepared. The difference in terminator composition to that used for the simulation studies above was made due to the availability of high purity MES, which at pH 8 has similar electrophoretic properties to  $\text{C}_8\text{SO}_3^-$ . Sample comprising 100 ppb of  $\text{I}^-$ ,  $\text{NO}_3^-$ ,  $\text{NO}_2^-$  and  $\text{SCN}^-$  was prepared in terminator and placed in the injection vial. A 25  $\mu\text{m}$  id fused-silica capillary was used for this work to match the simulated concentration of the leader/terminator composition used in

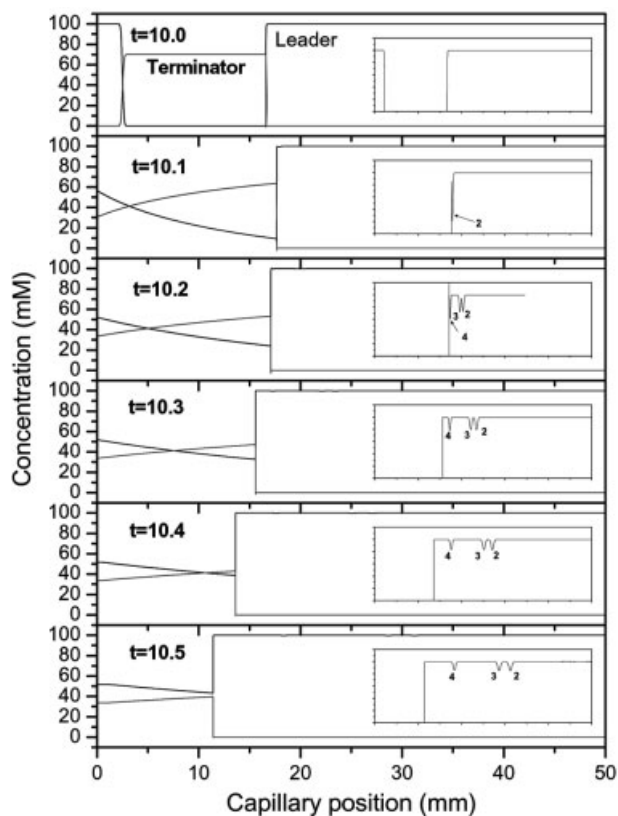


**Figure 4.** Computer simulations of the leader and terminator anions during the destacking process. Time 10.0 is the time after stacking and after the inlet vial has been changed to the electrolyte/leader. Peaks: 2,  $\text{NO}_2^-$ ; 3,  $\text{NO}_3^-$ ; 4,  $\text{SCN}^-$ . Other details as for Fig. 3.

the simulation studies without providing excessively high currents (the current when the capillary was filled with the leading electrolyte was approximately 60  $\mu\text{A}$ ). Sample was injected at a constant voltage of  $-20 \text{ kV}$  for times between 0.1 and 60 min, after which point the inlet vial was changed to leader/terminator for destacking and separation. Without the use of specialised equipment it is impossible to monitor the processes occurring inside the capillary but the current profile provides some insight into what is occurring. Figure 5 shows the current traces during sITP injection for injection times up to 60 min. The time at which the inlet vial was changed from sample/terminator to electrolyte/leader is indicated in each experiment with an arrow. It can be seen from these data that during stacking, the current initially goes down as the lower conductivity terminating ion enters the capillary taking the place of the higher conductivity leading ion. For injections 3 min or longer, the current approaches the same constant value indicating the number of ions entering and exiting the capillary is constant and is indicative of the generation of a sITP boundary. During destacking/separation after the inlet vial is changed from sample/terminator to leader/electrolyte the current rapidly

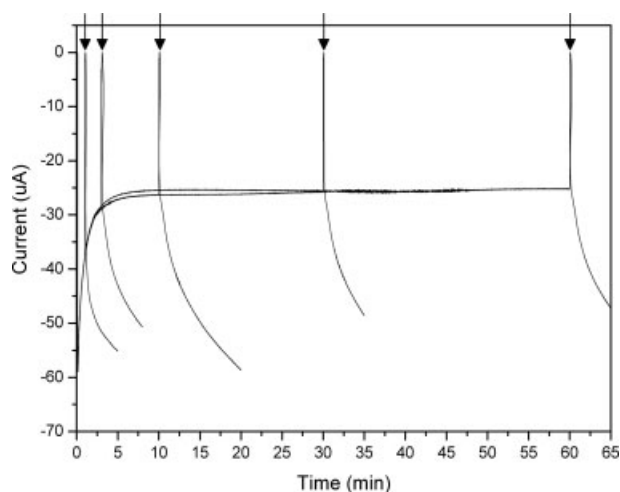


**Figure 5.** Experimental current trace for the stacking and destacking/separation of a mixture of four inorganic anions ( $I^-$ ,  $NO_2^-$ ,  $NO_3^-$  and  $SCN^-$ ) using a sITP boundary. Separations were performed in  $34.5\text{ cm} \times 25\text{ }\mu\text{m}$  id ( $26.0\text{ cm}$  to detector) fused-silica capillary. The leading/separation electrolyte was  $100\text{ mM Cl}^-$ , pH 8.05 buffered with Tris. Sample containing  $100\text{ ppb}$  of each anion was prepared in terminating electrolyte, which was  $100\text{ mM MES}$ , pH 8.05 buffered with Tris. Sample was injected at  $-20\text{ kV}$  for 1, 3, 10, 30 or 60 min, after which the inlet vial was changed to electrolyte/leader at the time indicated with the arrow and destacking/separation with a voltage of  $-28\text{ kV}$ .

increases as leading ions enter the capillary from the inlet vial and exchange for lower conductivity terminating ions, although it is interesting to note that 5 min after changing the inlet vial the current has still not reached a steady value indicating that there are still changes occurring within the capillary during the separation phase.

The corresponding absorbance trace is shown in Fig. 6a while Fig. 6b shows only the destacking/separation phase on individual scales for exactly the same separation. From Fig. 6a it can be seen clearly that the peak height increases considerably for  $NO_2^-$ ,  $NO_3^-$  and  $SCN^-$ , and as anticipated from the computer simulations, the increase in peak area is a linear function of the injection time ( $r^2 > 0.99$ , data not shown). Increasing the injection time from 0.1 to 60 min provides a 600-fold increase in peak area over the shorter 0.1 min injection. It is important to note that the peak area/height does not increase linearly for  $I^-$  illustrating one of the limitations of this system, namely, that it can only stack ions that have an electrophoretic mobility between the leader and terminator ions. Closer inspection of the separations in Fig. 6b reveals that the resolution decreases as the injection time is increased, although as the same sample was used for all injections, this is likely due to the system becoming overloaded due to high analyte concentrations. The time scale for the 60 min injection in Fig. 6b is also much shorter than that of the other separations. It is believed that this is due to additional hydrodynamic flow from the inlet to the outlet due to the large

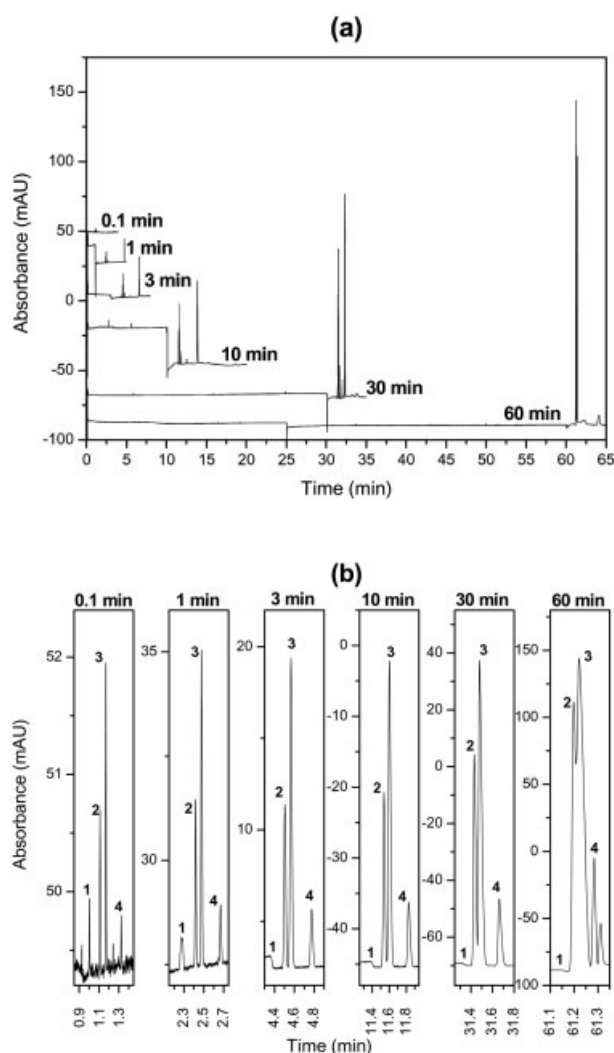


**Figure 6.** Absorbance traces for the sITP stacking and destacking/separation of the ions concentrated and separated in Fig. 4. (a) Shows the separations on the same scale, while (b) shows only the destacking/separation component on individual scales. Peaks: 1,  $I^-$ ; 2,  $NO_2^-$ ; 3,  $NO_3^-$ ; 4,  $SCN^-$ . Other conditions can be found in Fig. 5.

volume of liquid that is displaced during the continuous sample introduction. This was overcome with the application of high pressure (5 bar) on both the inlet and outlet vials in all subsequent studies presented here.

### 3.4 Starting conditions necessary for sITP stacking

In the results above, the capillary was initially filled with leading electrolyte while sample/terminator was placed in the inlet vial. It should also be possible to generate a sITP boundary if the capillary is filled with sample/terminator and only the outlet vial is filled with leader/electrolyte. The motivation behind this notion is two-fold. First, that there may be an improvement in sensitivity similar to that obtained using

large-volume sample stacking (LVSS), and second, that it will establish the sensitivity of the sITP injection to the initial setup conditions. Again, a dual approach of performing computer simulations as well as experimental data was undertaken. Figures 7 and 8 show the computer simulation column profiles of  $\text{SCN}^-$  and the simulated current profiles, while Figs. 9 and 10 show the experimental absorbance trace and current profiles. It can be seen from the figures that both the simulated and experimental current profiles (Figs. 8 and 10) show that when the capillary is initially filled with leader/electrolyte, the current decreases before stabilisation, while

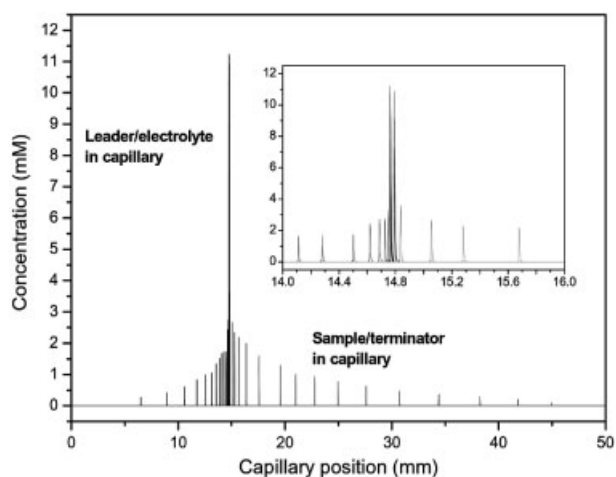


**Figure 7.** Computer simulations showing the sITP stacking of  $\text{SCN}^-$  when the capillary is filled with leader/electrolyte (stacked peaks moving to the right) or the capillary is filled with terminator/sample (stacked peaks moving to the left). Leading electrolyte is 100 mM  $\text{Cl}^-$ , pH 8.05 buffered with Tris, while the terminator is 100 mM MES, pH 8.05 buffered with Tris. All other conditions were the same as for Fig. 3.

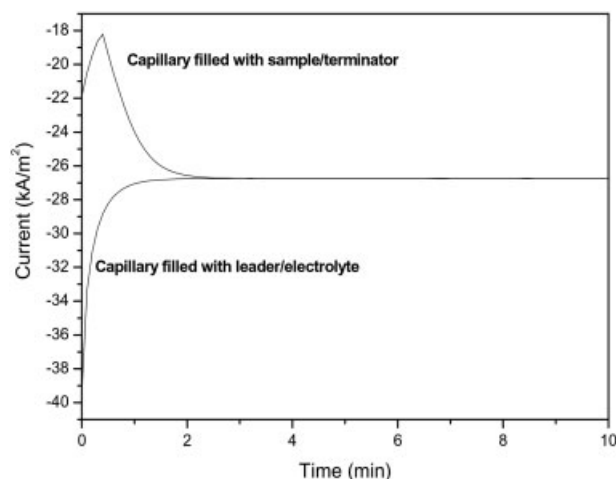


**Figure 8.** Current profiles from computer simulations when the capillary is filled with sample/terminator and the capillary is initially filled with leader/electrolyte. Conditions are the same as for Fig. 7.

when it is filled with terminator/sample, the current initially decreases before increasing and stabilising. In both cases, the stabilisation current is the same value from which it can be inferred that the sITP boundary is stabilised at the same position along the capillary. The current takes longer to stabilise when the capillary is filled with terminator/sample, most likely due to the farther distance that the ITP boundary has to travel before reaching the stabilisation point. Because of the time difference that it takes for the boundary to become stationary and the fact that the capillary is filled with sample, this could result in a practical difference in the sensitivity enhancement obtained with these two approaches. Examination of the simulated column profiles and the experimental absorbance traces (Figs. 7 and 9) shows that there is no major difference in sensitivity between filling the capillary with leader/electrolyte or terminator/sample. It is interesting to note that the computer simulation data in Fig. 7 indicate that there is a very minor difference in the position at which the sITP boundary is generated. While origin of this difference is unknown, it is unlikely to have a significant impact upon the sITP stacking system.

### 3.5 Analytical performance

Using the conditions in Fig. 6 and a 60 min injection, the detection limits of the three ions,  $\text{NO}_2^-$ ,  $\text{NO}_3^-$  and  $\text{SCN}^-$  were determined to be 0.13, 0.05 and 0.66 ppb, respectively, while the efficiencies (calculated from the difference between the migration time and the time the sITP injection was terminated) were approximately 150 000 plates/m. Intraday reproducibility ( $n = 5$ ) for migration times was less than 5% RSD while peak area was within 10%. Interday reproducibility ( $n = 5$ ) was slightly worse, with migration time reproducibility of 8% RSD and peak areas within 15%. While

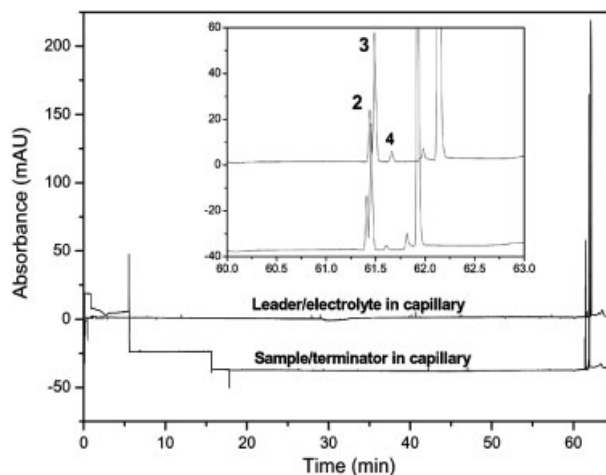


**Figure 9.** Experimental absorbance traces when the capillary is filled with leader/electrolyte and when the capillary is filled with terminator/sample. Peaks: 2,  $\text{NO}_2^-$ ; 3,  $\text{NO}_3^-$ ; 4,  $\text{SCN}^-$ . Conditions are the same as for Fig. 6.

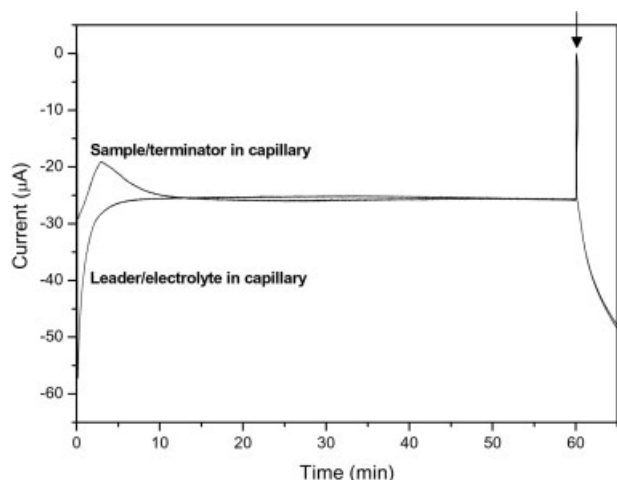


**Figure 10.** Experimental current trace from the experimental separations obtained in Fig. 9.

these results are worse than conventional CE, improved control of the EOF and the use of a climate-controlled laboratory should improve these results.

In comparison to other stacking methods developed for the selected inorganic ions, these detection limits are 10–50 times lower than those obtained by Quirino and Terabe [44] (1.8 ppb for  $\text{NO}_3^-$ ) using FESI, although their total analysis time was 15 min. They are also lower than the LODs obtained by Jandik and Jones (1.2 ppb for  $\text{NO}_2^-$ , 1.5 ppb for  $\text{NO}_3^-$ ) although it should be noted that they employed indirect detection using chromate and had a much shorter analysis time (5 min) [20]. In comparison to a conventional hydrodynamic injection, the sensitivity has been improved by 10 000. There is scope to improve the sensitivity further with the use of larger diameter capillaries, although that would require a reduction in the concentration of the leading and terminating electrolytes and was not examined in this work. As will be discussed in forthcoming papers, sITP stacking under field-amplified conditions provides even further improvements in sensitivity while sITP stacking can also be used to stack low mobility ions in the presence of a high concentration (100–500 mM) of leading ion.

#### 4 Concluding remarks

An online technique for the concentration of anions in CE based on the generation of a sITP boundary has been developed. By balancing the electrophoretic velocity of the ITP stacking boundary with that of the EOF it is possible to create a stationary stacking boundary that can be used for the unlimited concentration of charged analytes during electrokinetic injection provided that the sample contains a suitable terminator. Destacking and separation are facilitated by simply changing the inlet vial from sample to leader and destabilising the ITP boundary by migration of the leader through

the terminator zone. Computer simulations showed that the pH, and hence EOF, has a significant influence on the position at which the sITP boundary is stabilised, but not on its formation or preconcentration potential. Simulation and experimental results also demonstrated that sITP stacking is insensitive to the initial starting conditions, with similar results obtained if the capillary was filled with leader/electrolyte or with sample/terminator. The potential of this preconcentration approach was demonstrated with the 60 min sITP injection of three inorganic anions, with LODs 10 000 times lower than those obtained by hydrodynamic injection, and 10–50 times lower than those obtained by other stacking approaches.

*The author would like to acknowledge the Australian Research Council for funding this work through the provision of an Australian Postdoctoral Fellowship (DP0453223). Access to computing facilities at the Australian Partnership for Advanced Computing (APAC) and Tasmanian Partnership for Advanced Computing (TPAC) is also gratefully acknowledged.*

*The author has declared no conflict of interest.*

#### 5 References

- [1] Breadmore, M. C., *Electrophoresis* 2007, 28, 254–281.
- [2] Timerbaev, A. R., Hirokawa, T., *Electrophoresis* 2006, 27, 323–340.
- [3] Osbourn, D. M., Weiss, D. J., Lunte, C. E., *Electrophoresis* 2000, 21, 2768–2779.
- [4] Chen, X. G., Fan, L. Y., Hu, Z., *Electrophoresis* 2004, 25, 3962–3969.
- [5] Lin, C. H., Kaneta, T., *Electrophoresis* 2004, 25, 4058–4073.
- [6] Mikkers, F. E. P., Everaerts, F. M., Verheggen, T., *J. Chromatogr.* 1979, 169, 11–20.
- [7] Burgi, D. S., Chien, R. L., *Anal. Biochem.* 1992, 202, 306–309.
- [8] Gebauer, P., Thormann, W., Boček, P., *J. Chromatogr.* 1992, 608, 47–57.
- [9] Gebauer, P., Thormann, W., Boček, P., *Electrophoresis* 1995, 16, 2039–2050.
- [10] Aebersold, R., Morrison, H. D., *J. Chromatogr.* 1990, 516, 79–88.
- [11] Britz-Mckibbin, P., Kranack, A. R., Paprica, A., Chen, D. D. Y., *Analyst* 1998, 123, 1461–1463.
- [12] Park, S., Lunte, C. E., *J. Microcol. Sep.* 1998, 10, 511–517.
- [13] Zhao, Y. P., Lunte, C. E., *Anal. Chem.* 1999, 71, 3985–3991.
- [14] Haglund, H., Tiselius, A., *Acta Chem. Scand.* 1950, 4, 957–962.
- [15] Chien, R. L., Burgi, D. S., *J. Chromatogr.* 1991, 559, 141–152.
- [16] Hirokawa, T., Okamoto, H., Gaš, B., *Electrophoresis* 2003, 24, 498–504.
- [17] Quirino, J. P., Terabe, S., *Anal. Chem.* 2000, 72, 1023–1030.
- [18] Jung, B., Bharadwaj, R., Santiago, J. G., *Anal. Chem.* 2006, 78, 2319–2327.

- [19] Jung, B. G., Zhu, Y. G., Santiago, J. G., *Anal. Chem.* 2007, 79, 345–349.
- [20] Jandik, P., Jones, W. R., *J. Chromatogr.* 1991, 546, 431–443.
- [21] Preetz, W., *Talanta* 1966, 13, 1649–1660.
- [22] Preetz, W., Pfeifer, H. L., *Talanta* 1967, 14, 143–153.
- [23] Everaerts, F. M., Verheggen, T., Vandevenne, J. L. M., *J. Chromatogr.* 1976, 123, 139–148.
- [24] Shackman, J. G., Ross, D., *Anal. Chem.* 2007, 79, 6641–6649.
- [25] Gebauer, P., Boček, P., *Electrophoresis* 2000, 21, 3898–3904.
- [26] Mazereeuw, M., Spikmans, V., Tjaden, U. R., van der Greef, J., *J. Chromatogr. A* 2000, 879, 219–233.
- [27] Bergmann, J., Jaehde, U., Schunack, W., *Electrophoresis* 1998, 19, 305–310.
- [28] Bergmann, J., Jaehde, U., Mazereeuw, M., Tjaden, U. R., Schunack, W., *J. Chromatogr. A* 1996, 734, 381–389.
- [29] Enlund, A. M., Schmidt, S., Westerlund, D., *Electrophoresis* 1998, 19, 707–711.
- [30] Reinhoud, N. J., Tjaden, U. R., Vandergreef, J., *J. Chromatogr.* 1993, 641, 155–162.
- [31] Urbánek, M., Varenne, A., Gebauer, P., Křivánková, L., Gareil, P., *Electrophoresis* 2006, 27, 4859–4871.
- [32] Gong, M., Wehmeyer, K. R., Limbach, P. A., Heineman, W. R., *Anal. Chem.* 2006, 78, 6035–6042.
- [33] Horakova, J., Petr, J., Maier, V., Tesarova, E. *et al.*, *Electrophoresis* 2007, 28, 1540–1547.
- [34] Bier, M., Palusinski, O. A., Mosher, R. A., Saville, D. A., *Science* 1983, 219, 1281–7.
- [35] Saville, D. A., Palusinski, O. A., *AIChE J.* 1986, 32, 207–14.
- [36] Palusinski, O. A., Graham, A., Mosher, R. A., Bier, M., Saville, D. A., *AIChE J.* 1986, 32, 215–23.
- [37] Krivánková, L., Pantůčková, P., Gebauer, P., Boček, P. *et al.*, *Electrophoresis* 2003, 24, 505–517.
- [38] Thormann, W., Huang, T., Pawliszyn, J., Mosher, R. A., *Electrophoresis* 2004, 25, 324–337.
- [39] Mosher, R. A., Thormann, W., *Electrophoresis* 2002, 23, 1803–1814.
- [40] Mao, Q., Pawliszyn, J., Thormann, W., *Anal. Chem.* 2000, 72, 5493–5502.
- [41] Breadmore, M. C., Mosher, R. A., Thormann, W., *Anal. Chem.* 2006, 78, 538–546.
- [42] Breadmore, M. C., Macka, M., Avdalovic, N., Haddad, P. R., *Anal. Chem.* 2001, 73, 820–828.
- [43] Thormann, W., Caslavská, J., Mosher, R. A., *Electrophoresis* 1995, 16, 2016–2026.
- [44] Quirino, J. P., Terabe, S., *J. Chromatogr. A* 1999, 850, 339–344.